


Cryo-Temperature Pretreatment Increases the Pro-Angiogenic Capacity of Three-Dimensional Mesenchymal Stem Cells via the PI3K-AKT Pathway

Cell Transplantation
Volume 31: 1–12
© The Author(s) 2022
Article reuse guidelines:
sagepub.com/journals-permissions
DOI: 10.1177/09636897221106996
journals.sagepub.com/home/cll


Huasu Zhu^{1,2*}, Yong Zhuang^{3*}, Dong Li², Na Dong^{1,2},
Huixian Ma², Linghong Liu², Qing Shi², and Xiuli Ju^{2,3}

Abstract

To increase the potential and effectiveness of three-dimensional (3D) mesenchymal stem cells (MSCs) for clinical applications, this study explored the effects of short cryo-temperature pretreatment on MSC function. Adipose-derived MSCs (A-MSCs) were cultured via the ordinary monolayer method and 3D hanging drop spheroid method. When the cells adhered to the wall or formed a spheroid, they were subjected to hypothermic stress at 4°C for 1 h and then divided into three recovery periods at 37°C, specifically 0, 12, and 24 h. The control group was not subjected to any treatment throughout the study. Monolayer and 3D spheroid A-MSCs were analyzed via RNA sequencing after hypothermic stress at 4°C for 1 h. Subsequently, each group of cells was collected and subjected to phenotype identification via flow cytometry, and mRNA expression was detected via reverse transcription–quantitative polymerase chain reaction analysis. Western blot analysis was performed to analyze the PI3K-AKT signaling pathway in A-MSCs. The effects of A-MSCs on angiogenesis *in vivo* were examined using a chick chorioallantoic membrane assay. Transwell assays were performed to determine whether the culture supernatant from each group could induce the chemotaxis of human umbilical vein endothelial cells (HUVECs). Three-dimensional spheroid culture did not change the phenotype of A-MSCs. The expression of fibroblast growth factors, hepatocyte growth factors, and other angiogenesis-related factors in A-MSCs was upregulated. A-MSCs subjected to hypothermic stress promoted angiogenesis under both monolayer and 3D spheroid cultures. Moreover, the chemotaxis of HUVECs to the 3D spheroid culture supernatant increased substantially. Short cryo-temperature pretreatment could stimulate 3D spheroid A-MSCs and activate the PI3K-AKT pathway. This approach has the advantages of promoting angiogenesis and maintaining cell viability.

Keywords

adipose-derived mesenchymal stem cell, hypothermia, three-dimensional cultures, fibroblast growth factors, stem cell therapy

Introduction

The three-dimensional (3D) culture of mesenchymal stem cells (MSCs) avoids the space limitation of traditional two-dimensional culture¹. This exerts an effect on cytoskeleton maintenance and signal transduction promotion². Through the detection of genes and secretory factors, 3D-cultured MSCs can better simulate the actual situation *in vivo*. For clinical applications, the 3D culture of MSCs amplifies their immunomodulatory, anti-inflammatory, and microvascular-improving advantages³. Therefore, 3D culture has broader application prospects in MSC therapy.

Cells cultured in 3D show complex characteristics similar to those observed in their *in vivo* counterparts⁴, and 3D culture models have been proven to be the closest to natural conditions. MSCs have low immunogenicity and strong immune-regulation ability⁵ and play an important role in the

treatment of immune-related diseases such as osteoarthritis^{6,7}. Even during the COVID-19 pandemic, MSCs have played an active role in accelerating the recovery of critically ill

¹ Department of Pediatrics, Qilu Hospital, Cheeloo College of Medicine, Shandong University, Jinan, China

² Stem Cell and Regenerative Medicine Research Center, Qilu Hospital of Shandong University, Jinan, China

³ Department of Pediatrics, Qilu Hospital of Shandong University, Jinan, China

*Huasu Zhu and Yong Zhuang contributed equally to this work.

Submitted: March 12, 2022. Revised: May 16, 2022. Accepted: May 26, 2022.

Corresponding Author:

Xiuli Ju, Department of Pediatrics, Qilu Hospital of Shandong University, No. 107 Wenhua West Road, Jinan 250012, Shandong, China.
Email: jxlqly@163.com



patients and reducing case fatality⁸. The advantage of 3D culture methods for MSCs is that they can have higher dryness and maintain the cell phenotype⁹. In addition, exosome production with 3D culture is increased by 20-fold compared to that with traditional monolayer culture and results in higher biological activity¹⁰. The injection of MSCs into the articular cavity through microcryogels can considerably improve the survival and repair efficiency of cells in osteoarthritis treatment¹¹. Recently, the combination of MSC exosomes and 3D biomimetic materials has become a new technique for the treatment of osteoporosis¹². Moreover, adipose-derived MSCs (A-MSCs) can effectively promote osteochondral regeneration through 3D culture¹³. These applications confirm that the 3D culture of MSCs is the prevailing approach for cell therapy.

To fully realize the function of MSCs, physical and chemical methods have become the focus of current research. Pulsed electromagnetic fields can increase the functional activity of MSCs through the regulation of cytokines, growth factors, and angiogenesis, and this can improve the MSC-mediated regeneration of synovial tissue¹⁴. Heat shock pretreatment of MSCs can prevent chemotherapy-induced premature ovarian failure by reducing their rate of apoptosis¹⁵. Furthermore, interleukin-1 β pretreatment of MSCs can enhance their immunomodulatory properties, resulting in better efficacy against inflammatory diseases¹⁶. The pretreatment of MSCs with interferon (IFN- γ) enhances their immunosuppressive capacity by promoting M2 polarization of macrophages¹⁷. At present, there have only been a few studies on the effect of cryo-temperature pretreatment on gene expression and cell function in MSCs, and whether short cryo-temperature pretreatment can interfere with the clinical application of 3D spheroid A-MSCs remains unclear.

In this study, we used cryo-temperature pretreatment for 3D-cultured MSCs, aiming to further improve their treatment efficacy. The cell phenotype, cell viability, gene expression, and chemotactic ability of A-MSCs cultured *via* monolayer and 3D hanging drop methods were detected. An attempt was also made to combine cryo-temperature pretreatment with 3D culture to optimize the clinical application of MSCs.

Materials and Methods

Cell Culture

A-MSCs were prepared and identified as previously described¹⁸. The use of adipose tissue was approved by the Ethics Committee of Shandong University Qilu Hospital (Jinan, China). The cells were cultured in dishes with α -minimal essential medium (Gibco, Carlsbad, CA, USA) containing 10% fetal bovine serum (FBS; Gibco) and 1% penicillin-streptomycin (Gibco). To form spheroids, A-MSCs at passage 3–5 were cultured using the hanging drop method. Briefly, 1000 A-MSCs in 30 μ L growth medium per drop were plated in hanging drops and incubated for 6 h to form

spheroids. For subsequent experiments, the cell spheroids were incubated with 0.25% trypsin/ethylenediaminetetraacetic acid (EDTA) for 12 min (depending on the size of spheroids) with gentle pipetting once at 6 min. Human umbilical vein endothelial cells (HUVECs) were grown in endothelial cell medium (ScienCell, San Diego, CA, USA) containing 5% FBS, 1% endothelial cell growth supplement, and 1% penicillin-streptomycin. The cells were cultured at 37°C in a 5% CO₂ atmosphere.

Exposure to Hypothermia

To simulate hypothermic stress, monolayer and 3D spheroid A-MSCs were incubated for 1 h at 4°C. A set of samples were immediately analyzed (equilibration time of 0 h), whereas the other two groups of samples were transferred to an incubator for equilibration and recovery at 37°C for another 12 h and 24 h. We also collected the culture supernatant at various time points for HUVEC chemotaxis assay. The control group was cultured in a 37°C incubator for 24 h and tested at the same time as the experimental groups.

Phenotypic Analysis

Flow cytometry was performed to characterize A-MSCs and HUVECs. The following cell surface epitopes of A-MSCs were detected using anti-human CD29-phycoerythrin (PE) (TS2/16, 303004), CD31-PE (WM59, 303106), CD44-PE (IM7, 103024), CD45-fluorescein isothiocyanate (FITC) (HI30, 304006), CD73-PE (AD2, 344004), CD90-PE (5E10, 328110), CD105-PE (43A3, 323206), and CD271-PE (ME20.4, 345106). HUVECs were detected using anti-human CD31-PE. All antibodies were purchased from BioLegend (1:20 dilution; San Diego, CA, USA) and used according to the manufacturer's protocol. Flow cytometry was performed using the Guava easyCyte 6HT (EMD Millipore, Billerica, MA, USA), and the data were analyzed using FlowJo version 10 (Tree Star Inc., Ashland, OR, USA).

Three-Dimensional Spheroid Shaping and Morphological Analysis

Monolayer and 3D spheroid A-MSCs were subjected to scanning electron microscopy by WeiYa Bio-Technology Co., Ltd. (Jinan, Shandong, China). Samples were fixed using 2.5% glutaraldehyde solution for 3 h at 4°C. Microstructural characterization was performed using a high-resolution scanning electron microscope (Sigma300; Zeiss, Germany).

To observe the overall distribution of cells, digested A-MSCs were first stained with PKH26 using PKH26 Red Fluorescent Cell Linker Kits for General Cell Membrane Labeling (Sigma-Aldrich, St Louis, MO, USA). Prior to staining, PKH26 in diluent C was incubated in a water bath

at 37 °C for 15 min. A-MSCs stained with a cell membrane were cultured by the hanging drop method. After 24 h incubation in a 37°C incubator, the original position of the suspension was maintained for 4',6-diamidino-2-phenylindole (DAPI) staining. Next, 3D spheroid A-MSCs were subjected to hematoxylin and eosin staining for morphological evaluation. The spheroids were observed under a microscope (BX53; Olympus, Tokyo, Japan) and photographed (CellSens, Ver. 1.18; Tokyo, Japan).

Transcriptome Sequencing and Differentially Expressed Genes (DEGs) Analysis

Monolayer and 3D spheroid A-MSCs were incubated for 1 h at 4°C in the refrigerator. After hypothermic stress, the cells were immediately collected for RNA extraction using TRIzol (T9424-100mL; Sigma, USA). All RNA sequencing samples were commissioned and analyzed by Xiuyue Biol (Jinan, China).

DEGs between the four samples cryo-mono, cryo-3D, RT-mono, and RT-3D were identified via GEO2R online tools¹⁹ with $|\log_{2}FC| > 2$ and adjust P value < 0.05 . The DEGs between cryo-mono and cryo-3D specimen were recognized as dataset A. The DEGs of RT-3D and cryo-3D specimen were identified as dataset B. Dataset C was the DEGs of RT-mono and cryo-mono specimen. Then, the up-regulated DEGs and down-regulated DEGs between the three datasets were plotted in Venn software. Gene ontology analysis (GO) and Kyoto Encyclopedia of Gene and Genome (KEGG) pathways analysis were utilized to enrichment molecular function (MF), cellular component (CC), biological process (BP), and pathway of DEGs ($P < 0.05$).

RNA Extraction and Gene Expression Analysis

After 1 h of hypothermic stress, A-MSCs were collected after different incubation times. Total RNA was extracted using TRIzol reagent (T9424-100mL; Sigma, USA). First-strand cDNA was synthesized using 1 µg of total RNA in 10 µL of reverse transcriptase reaction mixture using the ReverTra Ace qPCR RT Master Mix kit (TOYOBO, Osaka, Japan) with specific primers. Reverse transcription-quantitative polymerase chain reaction (RT-qPCR) was performed using a Real Time Thermocycler (qTOWER3G; Analytik Jena AG, Germany), and detection was performed with SYBR Green Realtime PCR Master Mix (TOYOBO) in a 20-µL reaction mixture to detect the mRNA levels of cytokines. The primer sequences used for RT-qPCR are listed in Supplementary Table 1. The thermal cycling program was performed according to the manufacturer's protocol. Data were analyzed using Sequence Detection Software 1.4 (Applied Biosystems, CA, United States). The mRNA levels were normalized to the level of the control group as a reference, which was set to 1.

Western Blot Analysis

Protein extracts from A-MSCs (prior to and following different *in vitro* treatments) were prepared in RIPA lysis buffer (Solarbio, Beijing, China) with phosphatase/protease inhibitor (Beyotime, Shanghai, China). Then, proteins (60 µg) were separated on 7.5% acrylamide gels and transferred to polyvinylidene fluoride (PVDF) membranes (Millipore). The following commercially available antibodies and dilutions were used for western blotting: GAPDH (1:2000; 5174S, Cell Signaling Technology, United States), Phospho S473-AKT (1:1000; 4060S, Cell Signaling Technology, United States), AKT (1:1000; 9272S, Cell Signaling Technology, United States), Phospho Y607-PI3K (1:500; ab182651, Abcam, United States), and PI3K (1:1000; 4255S, Cell Signaling Technology, United States). After incubation with primary antibodies overnight at 4°C, the PVDF membranes were incubated with horseradish peroxidase-conjugated goat anti-rabbit (1:5000, ZB-2301, ZSGB-BIO, Beijing, China) secondary antibody for 1 h at 25°C. Proteins were visualized using enhanced chemiluminescence (JIAPENG, JP-K600plus, Shanghai, China). The band intensity was quantified using ImageJ software. All target protein signal intensities were normalized to GAPDH signals. Experiments were performed in triplicate.

Chick Chorioallantoic Membrane Assay of Angiogenic Activity

The effect of A-MSCs on angiogenesis was evaluated *in vivo* using a CAM vessel development assay. Seven-day-old eggs weighing 50–70 g were obtained from Shandong Experimental Breeder Farm of No Specific Pathogenic Chicken (Jinan, Shandong, China). Fertilized chicken eggs were acclimatized for 9 days in a standard egg incubator at 37°C and 60%–70% relative humidity. Before the experiment, A-MSCs (2×10^4 cells/egg) were embedded in 2.5% agar in advance. In brief, the MSCs were first suspended in pre-warmed medium and then mixed with an equal volume of 5% agar solution (111860; Biowest, Spain). After that, the agar was stabilized to a semi-solid state in a 37°C incubator. A circular window of 1–1.5 cm in diameter was opened aseptically on the eggshell, and the agar containing MSCs was grafted into the CAM. The window was sealed with medical tape and sealed with wax. The eggs were then placed in an incubator. After 72 h, the CAM was carefully removed and photographed using a Canon digital camera. Angiogenic index was defined as the area of visible blood vessel within a defined area of 9.6 cm². Assays for each test sample were performed using five eggs. The area of blood vessels was measured using the ImageJ software (National Institutes of Health, Bethesda, MD, USA).

Transwell Chemotaxis Assay

HUVECs (2×10^4) were seeded in alpha-minimal essential medium supplemented with 5% FBS in the upper chamber. The lower chamber was filled with culture supernatants collected at 0, 12, and 24 h after exposure to hypothermia. After incubation for 18 h, the cell membrane surface was wiped off with cotton swabs. The upper chamber was washed, fixed, dyed with 0.1% crystal violet, and photographed. Cell migration ability was determined by counting the number of cells in the lower chamber.

Statistical Analysis

All data are presented as the mean \pm SD of three biological repeats experiments. Statistical analyses were performed by one-way analysis of variance (ANOVA) or two-way ANOVA following Tukey's multiple comparisons test. Differences were considered significant at a probability level of $P < 0.05$. Statistical analyses were performed using Prism 8 (GraphPad Software Inc., San Diego, CA, USA).

Results

Hanging Drop Culture Does Not Change the Phenotype of A-MSCs

Through flow cytometry, we examined the consistency of the immunophenotype of A-MSCs before and after hanging drop culture. The results revealed that the A-MSCs showed the typical immunophenotypes of MSCs. Both A-MSCs grown in a monolayer and 3D spheroid cultures highly expressed the MSC markers CD29, CD44, CD73, CD90, and CD105 but did not express the endothelial cell markers (CD31), hematopoietic markers (CD45), and differentiated activated effector cell markers (CD271) (Fig. 1A).

Characteristics of Spheroids

P3 A-MSCs were cultured in a dish using the hanging drop method (Fig. 2). After 24 h, the MSCs were observed to form spheres with a diameter of approximately 50 μ m under a light microscope (Fig. 3A). Immunofluorescence (Fig. 3B) and hematoxylin and eosin (Fig. 3C) staining showed that the cells in the spheroids closely adhered to each other and were more compact than those in the monolayer culture. Scanning electron microscopy results (Fig. 3D) showed that, compared with that in the monolayer culture, the volume of each cell in the 3D spheroid was smaller (approximately a quarter of that in the monolayer culture) and the nucleus was larger. The cells in the spheroid formed dense connections and cannot be separated into individual cell boundaries. Through immunofluorescence staining, we were able to preliminarily judge that there were approximately 100 cells in each 3D spheroid according to the density of our culture.

Effect of Culture Method and Cryo-Temperature Stress on Transcriptional of A-MSCs

Considering the uniqueness of the 3D hanging drop culture, we performed transcriptomic analysis on monolayer and 3D spheroid A-MSCs before and after hypothermic stress. Top five significantly enriched biological processes between the dataset A and dataset C were condensed DNA-dependent DNA replication, regulation of cell cycle phase transition, cell cycle G1/S phase transition, negative regulation of phosphorylation, and G1/S transition of mitotic cell cycle (Fig. 4C). KEGG pathway analysis using the KEGG pathway database (www.genome.jp/kegg/pathway.html) identified the top five most significantly enriched pathways between the dataset B and dataset C culture groups, which were PI3K-AKT signaling pathway, axon guidance, proteoglycans in cancer, human T-cell leukemia virus 1 infection, and salmonella infection (Fig. 4D). These results indicated that cryo-temperature stress significantly enriched in cell proliferation-related signaling pathways and affected cell cycle. Therefore, preliminary RNA-Seq results showed that cryo-temperature stress and culture method significantly altered the gene expression of A-MSCs.

Hypothermic Stress Causes Changes Differential Expression of FGF and Activates the PI3K-AKT Pathway

Based on previous transcriptomic results, we analyzed the types of the differentially expressed genes. We further verified the expression of mRNAs related to angiogenesis and neurotrophic activity by RT-qPCR. Among the monolayer groups, the mRNA levels of acid FGF (AFGF), basic FGF (BFGF), nerve growth factor (NGF), brain-derived neurotrophic factor (BDNF), and stem cell factor (SCF) at 12 h were increased compared with those at 0 h ($*P < 0.05$, $**P < 0.01$, Fig. 5A–D and H). Among the 3D spheroids group, similarly, the mRNA levels of AFGF and BFGF were increased at the same time point ($*P < 0.05$, $**P < 0.01$, $***P < 0.001$, Fig. 5A and B). In addition, in the 3D spheroid culture, the mRNA levels of HGF, matrix metalloproteinase (MMP), and insulin-like growth factor 1 (IGF-1) increased at 12 h compared with those at 0 h and SCF increased maximum at 0 h ($**P < 0.01$, $*P < 0.05$, Fig. 5E–H). Specifically, the levels of NGF and BDNF in the 3D spheroid culture at 12 h were significantly increased compared with those at 0 h ($*P < 0.05$, $***P < 0.001$, Fig. 5C–D). Besides, the mRNA level of ubiquinone oxidoreductase subunit S6 (NDUFS6) was increased at 0 h compared with at 12 h in both monolayer groups and the 3D spheroid culture ($**P < 0.01$, $***P < 0.001$, Fig. 5I). In order to confirm the regulatory mechanism of A-MSCs after hypothermic stress. Furthermore, based on the aforementioned KEGG-enriched

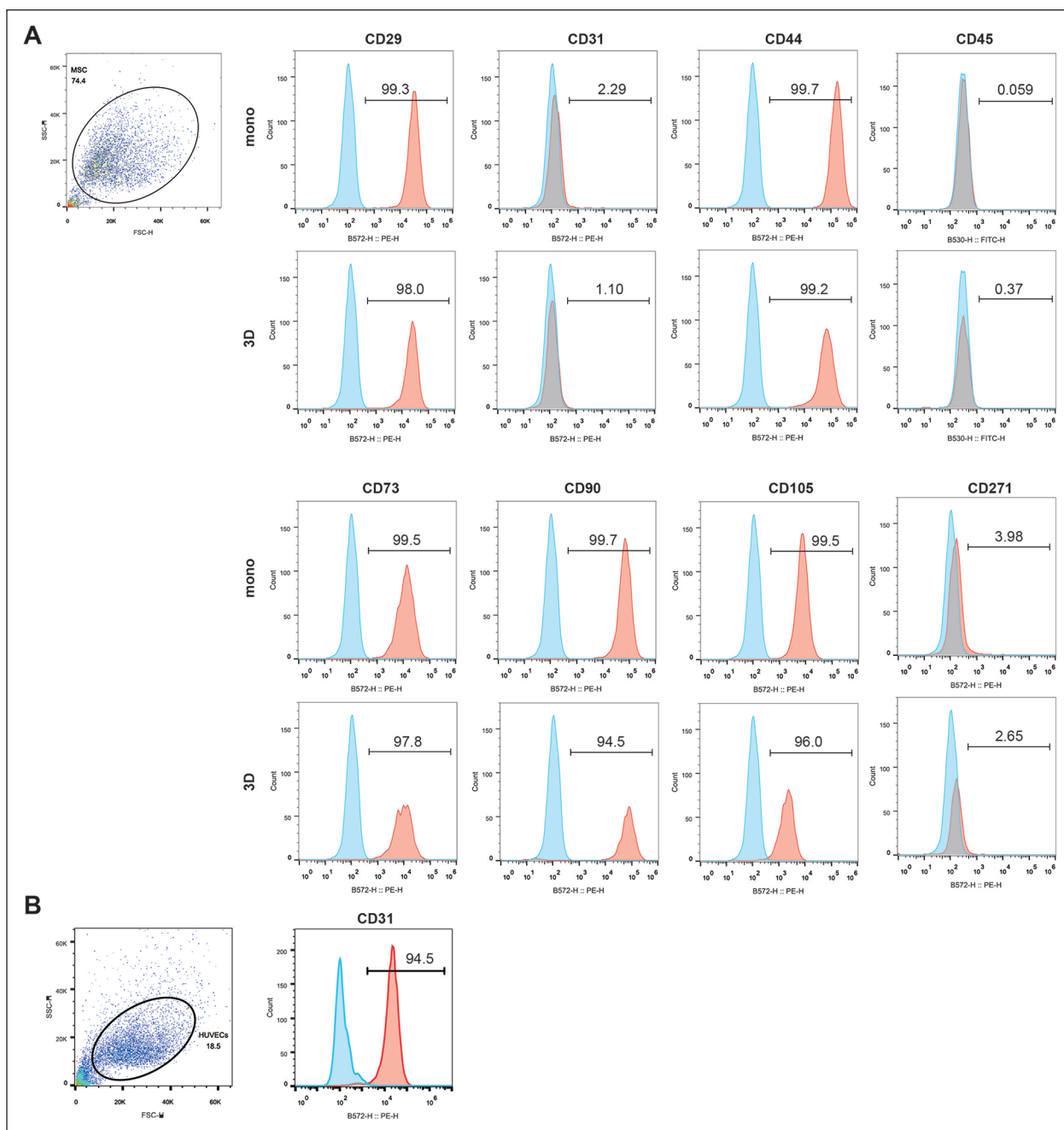


Figure 1. Immunophenotypes of A-MSCs and HUVECs as determined by flow cytometry. (A) Immunophenotype of monolayer and 3D spheroid A-MSCs. The expression of positive stem markers CD29, CD44, CD73, CD90, and CD105 and negative stem markers CD31, CD45, and CD271. (B) Phenotypic identification of HUVECs. The isolated cultured cells were stained with endothelial cell marker CD31. A-MSCs: Adipose-derived mesenchymal stem cells; HUVECs: human umbilical vein endothelial cells.

pathways, we examined the protein level of phospho-PI3K, PI3K, phospho-AKT, and AKT. The protein expression ratio of phospho-PI3K/PI3K and phospho-AKT/AKT was significantly increased in the monolayer groups at 12 h compared with control after hypothermic stress ($*P < 0.05$, Fig. 5K and L). In the 3D spheroid culture, however, these increases were significant at 0 h ($*P < 0.05$, $**P < 0.01$, Fig. 5M and N).

A-MSCs Subjected to Hypothermic Stress Promote Angiogenesis in CAM Model

To explore whether exposure to hypothermic stress affects the angiogenic activity of A-MSCs, we conducted a CAM assay *in vivo*. Among the monolayer groups, the cells incubated for 12 h after hypothermic stress significantly induced neo-vascularization compared with the control ($***P < 0.001$,

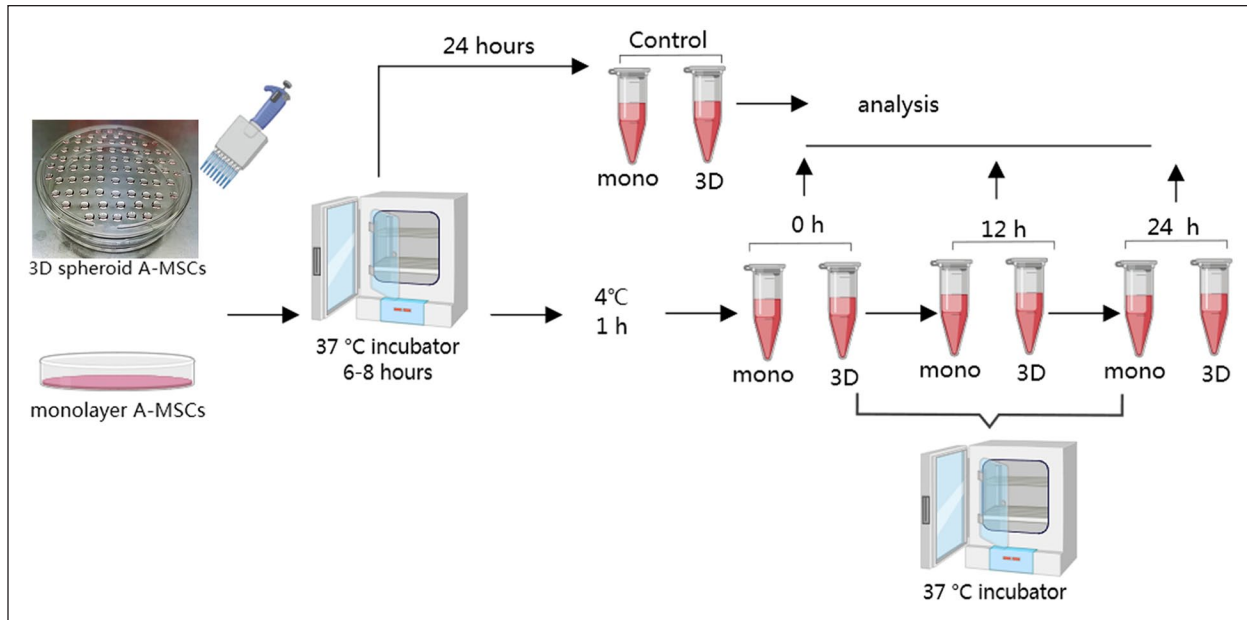


Figure 2. Schematic diagram of the experimental design: the 3D spheroid and monolayer groups were allowed to form spheroids or adhere to the dish wall, respectively, in a 37°C incubator for 6–8 h. After 1 h of hypothermic stress treatment at 4°C, the cells in both groups were further incubated at 37°C for different periods: 0, 12, and 24 h. The control group did not undergo any treatment until the end. A-MSCs: Adipose-derived mesenchymal stem cells.

Fig. 6A and B) (bule). Moreover, neovascularization in the 12 h group was the highest compared with that in the 0 and 24 h groups ($^{##}P < 0.01$, Fig. 6B) (bule). However, among the 3D spheroids groups, compared with that in the control, the highest neovascularization was shown by A-MSCs collected immediately after exposure to hypothermia at 4°C for 1 h ($^{**}P < 0.01$, Fig. 6B) (red), and good neovascularization was observed after 12 h of recovery at 37°C ($^{*}P < 0.05$, Fig. 6B) (red). Compared with the 12 h group, the 24 h group showed a lower degree of angiogenesis ($^{#}P < 0.05$, Fig. 6B) (red) and no difference from the control group.

Three-Dimensional Spheroid A-MSCs Subjected to Hypothermic Stress Can Better Induce HUVEC Migration

RT-qPCR analysis revealed that the expression levels of angiogenesis- and nutrition-related factors in 3D spheroid and monolayer A-MSCs changed after hypothermic stress. Next, we observed the ability of the culture supernatant to induce the chemotaxis of HUVECs in Transwell assays. Before the experiment, we identified the characteristics of HUVECs by flow cytometry. The expression of the endothelial cell marker CD31 was determined to be as high as 98% (Fig. 1B). Transwell assay results showed that the number of migrating cells at each time point in the 3D spheroid groups was greater than that in the monolayer groups ($^{*}P < 0.05$, Fig. 7A and B). Among the monolayer groups, the HUVEC

migration ability of the 12 h group was higher than that of the 0 and 24 h groups ($^{#}P < 0.05$, Fig. 7B) (bule). However, among the 3D spheroids group, the highest chemotaxis of HUVECs was shown by the supernatant collected immediately after hypothermic treatment at 4°C for 1 h compared with that in the control and 12 h groups ($^{##}P < 0.01$ and $^{#}P < 0.05$, respectively, Fig. 7B) (red).

Discussion

In nature, adipose tissue adjusts the metabolic state of mammals according to temperature changes to maintain a constant body temperature²⁰. Based on this phenomenon, changes in temperature are more likely to cause changes in the function of A-MSCs. This is also the reason why we selected A-MSCs as the research object of cryo-temperature stress testing. In recent years, 3D cell culture based on agarose, collagen, fibronectin, gelatin, and laminin has become a new approach for cell therapy²¹. Among them, the advantages of the hanging drop method are its simple operation and high repeatability. Another important advantage of this method is the avoidance of contamination of exogenous proteins in the collagen scaffold. In this study, we successfully constructed 3D spheroid A-MSCs *via* the hanging drop method. MSCs can form spheroids in 6 h. Under electron and light microscopy, A-MSCs obtained from hanging drop culture showed a dense spherical structure and stable cell number, and this did not change the immunophenotype of A-MSCs.

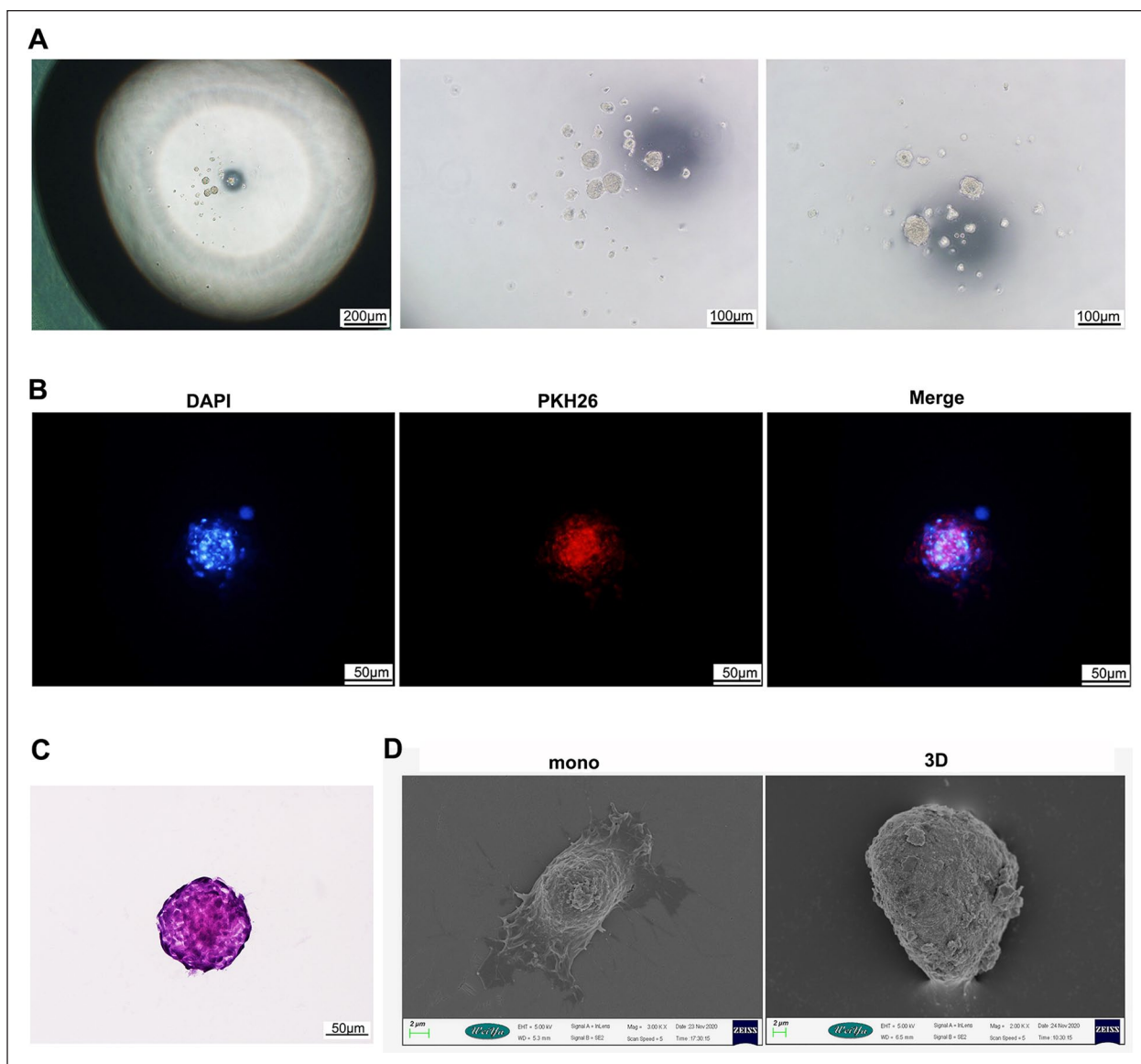


Figure 3. Morphology of 3D multicellular spheroid A-MSCs. (A) Morphology of the 3D spheroid under a light microscope. (B) Morphology of the 3D spheroid under PKH26 and DAPI immunofluorescence staining (microscope magnification: 200 \times). (C) Hematoxylin and eosin staining of the 3D spheroid (microscope magnification: 200 \times). (D) Morphology of monolayer and 3D spheroid A-MSCs under a scanning electron microscope. A-MSCs: Adipose-derived mesenchymal stem cells; DAPI, 4',6-diamidino-2-phenylindole.

Improving microcirculation is an important therapeutic basis for MSCs. Therefore, we first tested the angiogenesis-promoting ability of MSCs pretreated using short hypothermic periods. We used the CAM assay to examine the effect of different culture methods and incubation times on the angiogenic activity of A-MSCs *in vivo*. The CAM assay was first used in the study of neovascularization²². As a unique *in vivo* support environment, CAM assays are not only suitable for studying angiogenesis but also have advantages for studying tumorigenesis²³. Angiogenesis was significantly promoted in the monolayer group after 12 h of incubation at 37°C. However, the 3D spheroid group showed

significant increases in angiogenic activity at both 0 and 12 h after exposure to hypothermia.

Subsequently, a Transwell assay was performed with HUVECs to verify the chemotaxis-inducing activity of the culture supernatants sampled at different time points. Similar to the results of the CAM assays, compared with that in the monolayer groups, the 3D spheroid groups displayed evident increases in the chemotaxis of HUVECs at various time points. It is worth noting that the chemotactic ability of monolayer and 3D spheroid A-MSCs was observed after 12 h of incubation at 37' and immediately after exposure to hypothermic stress, respectively. However, it should be

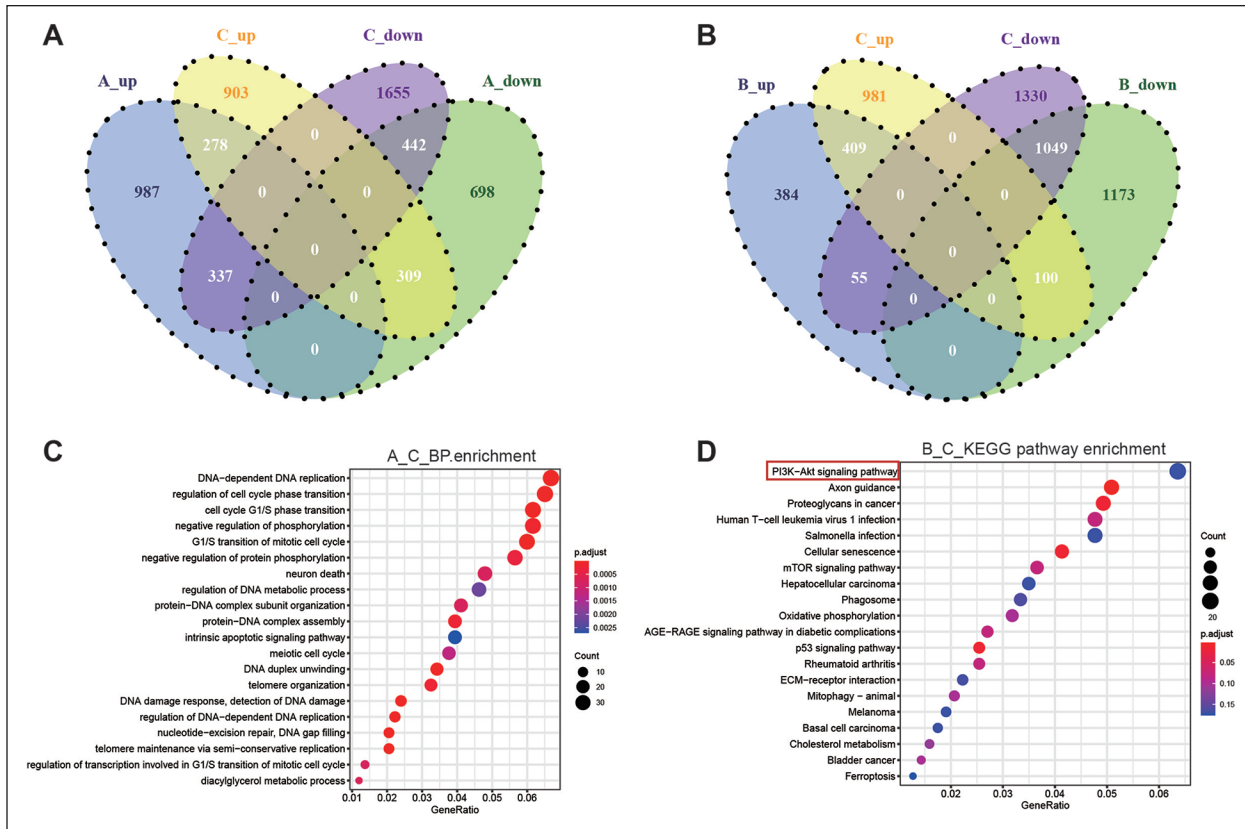


Figure 4. Authentication of DEGs in the three datasets ([A] cryo-mono vs. cryo-3D, (B) RT-3D vs. cryo-3D and (C) RT-mono vs. cryo-mono) through Venn diagrams software. Different color meant different datasets. (A) Venn diagrams containing lists of up-regulated and down-regulated DEGs in dataset A and C ($|\log_{2}FC| > 2$). (B) Venn diagrams containing lists of up-regulated and down-regulated DEGs in dataset B and C ($|\log_{2}FC| > 2$). (C) Biological processes enrichment diagram of Q values for single group GO items in dataset A and C. (D) Distribution diagram of Q values for the top twenty significantly enriched pathways of dataset B and C. BP: biological process; DEG: Differentially Expressed Genes; DNA: deoxyribonucleic acid; GO: gene ontology; KEGG: Kyoto Encyclopedia of Gene and Genome; RT: reverse transcription; mTOR: mammalian target of rapamycin; ECM: extracellular matrix.

noted that in the *in vivo* CAM assay, the overall angiogenic activity of 3D spheroid A-MSCs did not differ from that of the monolayer groups. This is inconsistent with the results of the *in vitro* Transwell assay. This inconsistency between the *in vivo* and *in vitro* experiments might be caused by the internal immune system of chicken embryos²⁴, considering that A-MSCs, as an exogenous biological stimulus, are a challenge to the immune system of chicken embryos in the developmental stage. However, some studies have shown that chicken embryos lack a fully functional immune system during the development of the vascular system²⁵. This will be examined further in our future studies.

Similar to the results of several cell function experiments, the RT-qPCR results showed upregulation of *FGF*, *HGF*, *MMP*, and *SCF* genes after 12 h of recovery at 37°C. The FGF family has the function of promoting angiogenesis and regulating cell growth and motility^{26,27}. Matrix metalloproteinases (MMPs) can resist extracellular matrix fibrosis, reduce adhesion inhibition between MSCs, and improve the microenvironment²⁸. SCF is the key trophic factor to

promote MSCs to resist stress, making them have superior anti-apoptotic and pro-proliferative effects²⁹. Considering the previously discovered advantages of 3D cultures, this result was also expected. Additionally, Yuelin Zhang et al.³⁰ confirmed that depressed NDUFS6 and MSC aging interact in a manner of reciprocal causation. In this study, A-MSCs treated with cryo-temperature pretreatment did not show a significant decrease in NDUFS6. Moreover, the RNA-Seq-enriched signaling pathways suggested that the PI3K-AKT signaling pathway of A-MSCs was significantly changed after exposure to hypothermia. The PI3K-AKT pathway plays an important role in promoting angiogenesis, maintaining cell proliferation, and promoting cell migration. Cardiac mesenchymal stromal cell-derived extracellular vesicles are involved in endogenous cardiac repair by promoting angiogenesis through the activation of PI3K-AKT³¹. Certain microRNAs can also promote maxillofacial bone regeneration via the PI3K-AKT pathway³². Moreover, blocking the PI3K-AKT signaling pathway of bone marrow MSCs can inhibit tumor cell proliferation and migration³³. Our data

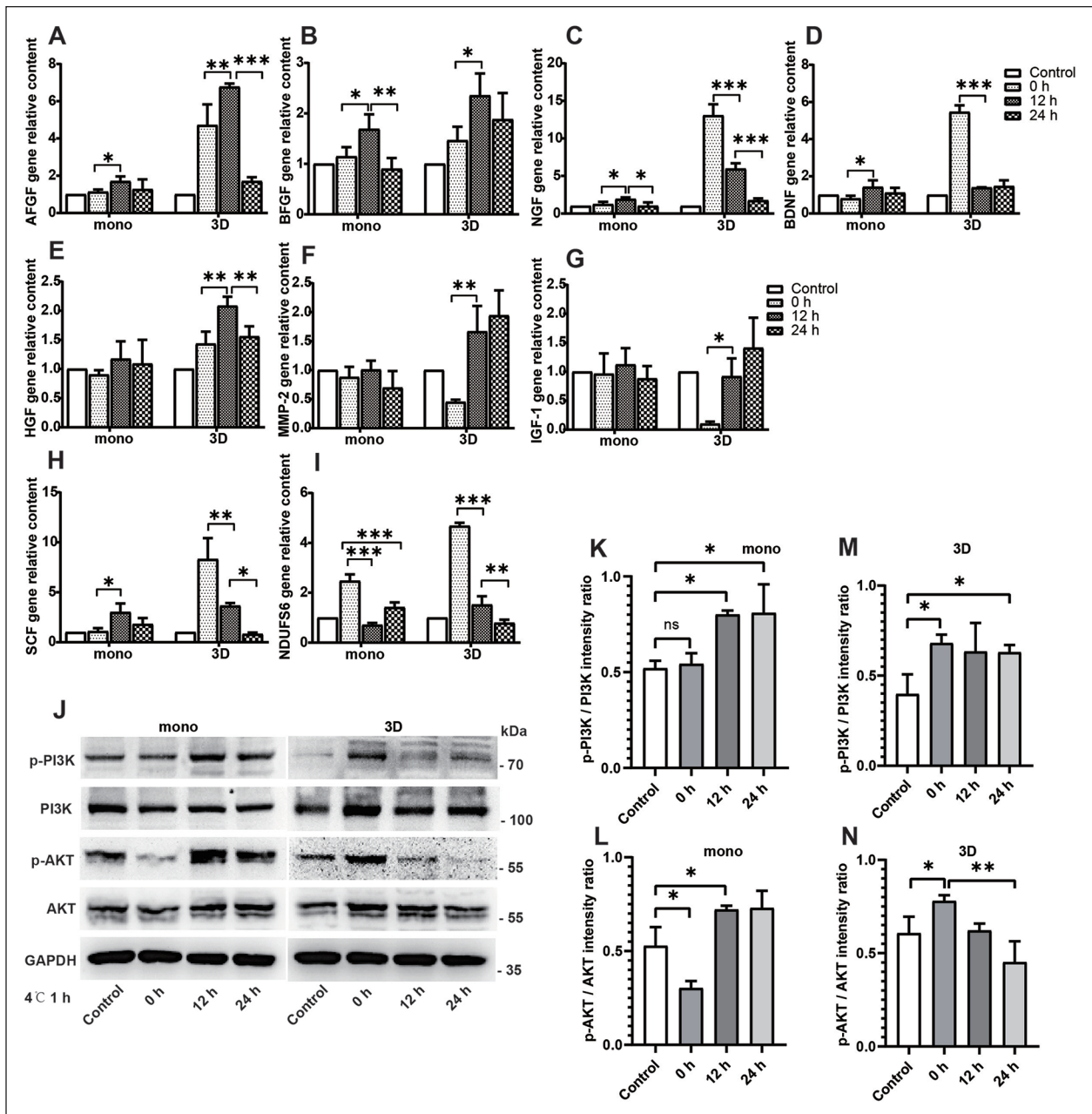


Figure 5. Under hypothermic stress, mRNA was differentially expressed between monolayer and 3D spheroid A-MSCs, and the PI3K-AKT pathway was activated. (A–I) The RT-qPCR experiment verifies that the genes AFGF, BFGF, NGF, BDNF, HGF, MMP-2, IGF-1, SCF and NDUFS6 were differentially expressed at the mRNA level. (J–N) Western blot and statistical analyses of p-PI3K, PI3K, p-AKT, and AKT in monolayer or 3D spheroid A-MSCs. GAPDH was used as a loading control. A-MSCs: adipose-derived mesenchymal stem cells; RT-qPCR: reverse transcription-quantitative polymerase chain reaction. All data are expressed as the mean \pm SD ($n=3$, $*P < 0.05$, $**P < 0.01$, $***P < 0.001$), and were analyzed by one-way ANOVA. p-PI3K/PI3K: phospho-phosphatidylinositol 3-kinase; p-AKT/AKT: phospho-serine/threonine kinase; GAPDH: Glyceraldehyde-3-phosphate dehydrogenase.

strongly suggest that cryo-temperature stress applied to 3D spheroid MSCs, without blocking the PI3K-AKT pathway, reduces PI3K, and AKT phosphorylation, which remains activated after recovery at 37°C.

Mild hypothermia alleviates hypoxic ischemic damage and increases tolerance to hypoxia *via* small ubiquitin-like modifier proteins of marrow-derived MSCs^{34,35}. Although

hypothermia reduces the gene expression of vascular endothelial growth factor, it does not affect the differentiation or apoptosis of MSCs exposed to hypoxia³⁶. It can be seen that cryo-temperature pretreatment can enable MSCs to realize their potential under harsh conditions. This is also similar to the results of our present study. However, the A-MSCs extracted in this study have limitations in practical clinical

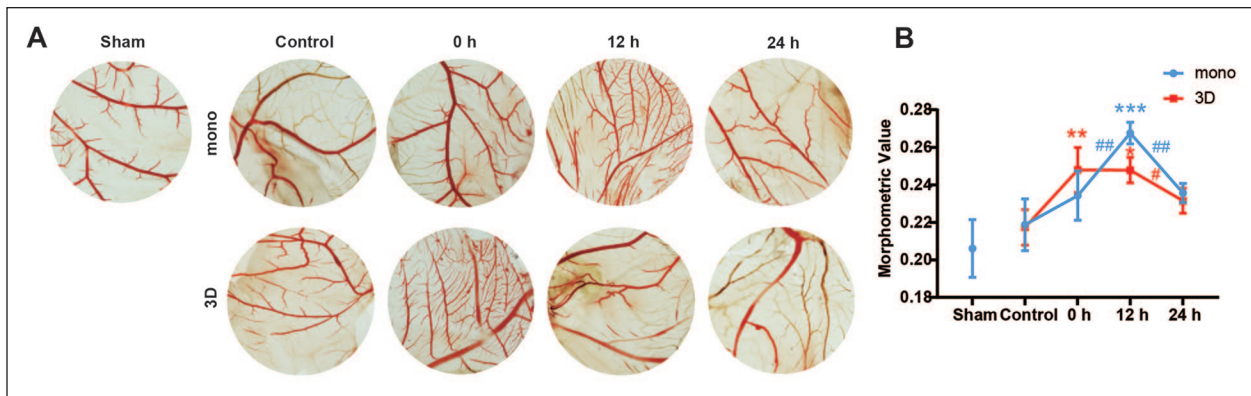


Figure 6. Monolayer and 3D spheroid A-MSCs were embedded on CAM to test for angiogenic activity. (A) Representative photos of vascularization on CAM treated with monolayer and 3D spheroid A-MSCs. The selected area is locked at 9.6 cm². (B) Morphological quantification revealed that the monolayer group showed the highest angiogenic activity after the temperature was restored to 37 °C for 12 h (n=5, ***P < 0.001). The 3D spheroid group displayed good angiogenic activity from 0 to 12 h (n=5, *P < 0.05, **P < 0.01). The data are expressed as the mean ± SD, and were analyzed by one-way ANOVA. A-MSCs: adipose-derived mesenchymal stem cells; CAM: chorioallantoic membrane.

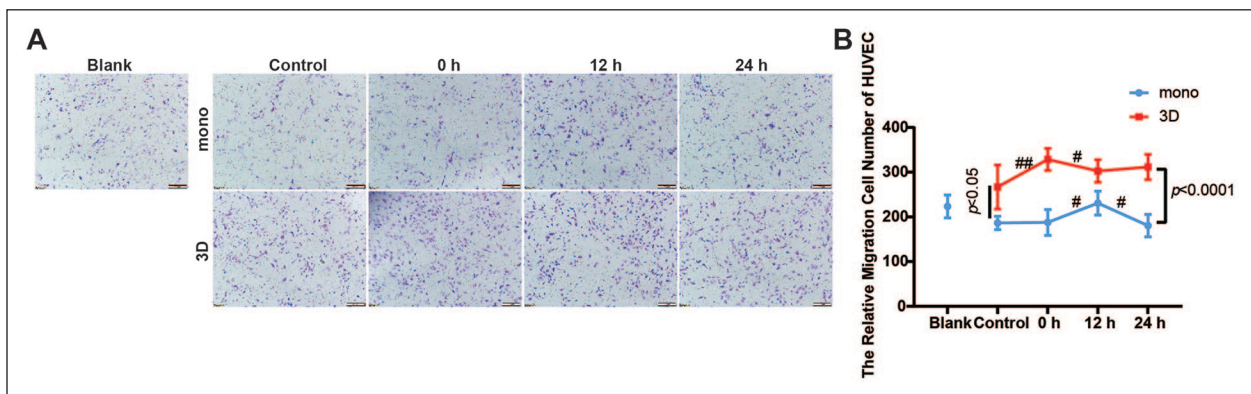


Figure 7. Culture supernatant of the 3D spheroid group showed obvious migrated HUVECs due to chemotaxis. (A) Two representative pictures of cell migration at different time periods. Microscope magnification: 100×. (B) Relative number of HUVECs that migrated to monolayer and 3D spheroids A-MSCs. The data are expressed as the mean ± SD (n=3, #P < 0.05, ##P < 0.01), and were analyzed by two-way ANOVA. A-MSCs: Adipose-derived mesenchymal stem cells; HUVECs: human umbilical vein endothelial cells.

applications. MSCs from induced pluripotent stem cells (iPSCs) that overcome batch-to-batch heterogeneity, have been used in refractory graft-versus-host-disease (GVHD) in clinical trials^{37,38}. This is also the key to improving MSCs yield and preventing stem cell senescence in the clinical treatment. Strikingly, after short-term stress at 4°C, the function of 3D spheroid A-MSCs could be activated immediately, without the need for incubation at 37°C. This further confirms that 3D spheroid culture can increase the stability of MSCs under special conditions. However, whether 3D spheroid MSCs can resist long-term hypothermic stress needs further study.

In conclusion, 3D spheroid MSCs after short cryo-temperature pretreatment can enhance the expression of angiogenic and neurotrophic-related factors, activate the PI3K-AKT pathway, and better maintain cell pro-angiogenic capacity. This method not only maintains the immune

characteristics of MSCs but also stimulates the functions of MSCs to a certain extent. At the same time, our results show that the hanging drop method is a simple and highly reproducible way to culture A-MSCs in three dimensions. In further studies, we will validate the function of 3D spherical MSCs in animal models.

Acknowledgments

The authors are grateful to Dr. Ju XL for help with regard to funding support. We also thank Li D for inspiring discussions.

Author Contributions

Zhu HS, Zhuang Y and Dong N completed the experiment and analyzed the results statistically. Li D, Ma HX and Ju XL proposed the design and conception of the experiment. Shi Q and Liu LH have plotted the chart. The manuscript was drafted and revised by Zhu HS and Zhuang Y. All authors have approved the final article.

Ethical Approval

This study was approved by the Ethics Committee of Shandong University Qilu Hospital (approval no KYLL-2019[KS]-086).

Statement of Human and Animal Rights

All procedures in this study were conducted following the protocol approved by “the Ethical Committee of Shandong University Qilu Hospital” and complied with the recommendations of the Declaration of Helsinki.

Statement of Informed Consent

Written informed consent was obtained from each adipose tissue donor.

Declaration of Conflicting Interests

The author(s) declared no potential conflicts of interest with respect to the research, authorship, and/or publication of this article.

Funding

The author(s) disclosed receipt of the following financial support for the research, authorship, and/or publication of this article: This work was supported by grants from Rongxiang Regenerative Medicine Foundation of Shandong University (No. 2019SDRX-18); Clinical Practical New Technology Development Fund of Qilu Hospital of Shandong University (No. 2019-0057); Clinical Research Center of Shandong University (No. 2020SDUCRCA010); and Natural Science Foundation of Shandong Province (No. ZR2020MH063).

ORCID iDs

Dong Li  <https://orcid.org/0000-0002-6496-4605>

Xiuli Ju  <https://orcid.org/0000-0001-5464-3106>

Supplemental Material

Supplemental material for this article is available online.

References

- Pittenger MF, Discher DE, Peault BM, Phinney DG, Hare JM, Caplan AI. Mesenchymal stem cell perspective: cell biology to clinical progress. *NPJ Regen Med.* 2019;4:22.
- Guo Y, Du S, Quan S, Jiang F, Yang C, Li J. Effects of biophysical cues of 3D hydrogels on mesenchymal stem cells differentiation. *J Cell Physiol.* 2021;236(4):2268–75.
- Kim BC, Kwack KH, Chun J, Lee JH. Comparative transcriptome analysis of human adipose-derived stem cells undergoing osteogenesis in 2D and 3D culture conditions. *Int J Mol Sci.* 2021;22(15):7939.
- Antoni D, Burckel H, Josset E, Noel G. Three-dimensional cell culture: a breakthrough in vivo. *Int J Mol Sci.* 2015;16(3):5517–27.
- Jiang W, Xu J. Immune modulation by mesenchymal stem cells. *Cell Prolif.* 2020;53(1):e12712.
- Cosenza S, Toupet K, Maumus M, Luz-Crawford P, Blanc-Brude O, Jorgensen C, Noel D. Mesenchymal stem cells-derived exosomes are more immunosuppressive than microparticles in inflammatory arthritis. *Theranostics.* 2018;8(5):1399–1410.
- Lee YH, Park HK, Auh QS, Nah H, Lee JS, Moon HJ, Heo DN, Kim IS, Kwon IK. Emerging potential of exosomes in regenerative medicine for temporomandibular joint osteoarthritis. *Int J Mol Sci.* 2020;21(4):1541.
- Klimczak A. Perspectives on mesenchymal stem/progenitor cells and their derivatives as potential therapies for lung damage caused by COVID-19. *World J Stem Cells.* 2020;12(9):1013–22.
- Li J, Chen T, Huang X, Zhao Y, Wang B, Yin Y, Cui Y, Zhao Y, Zhang R, Wang X, Wang Y, et al. Substrate-independent immunomodulatory characteristics of mesenchymal stem cells in three-dimensional culture. *PLoS ONE.* 2018;13(11):e0206811.
- Haraszti RA, Miller R, Stoppato M, Sere YY, Coles A, Didiot MC, Wollacott R, Sapp E, Dubuke ML, Li X, Shaffer SA, et al. Exosomes produced from 3D cultures of MSCs by tangential flow filtration show higher yield and improved activity. *Mol Ther.* 2018;26(12):2838–47.
- Xing D, Liu W, Wang B, Li JJ, Zhao Y, Li H, Liu A, Du Y, Lin J. Intra-articular injection of cell-laden 3D microcryogels empower low-dose cell therapy for osteoarthritis in a rat model. *Cell Transplant.* 2020;29:963689720932142.
- He XY, Yu HM, Lin S, Li YZ. Advances in the application of mesenchymal stem cells, exosomes, biomimetic materials, and 3D printing in osteoporosis treatment. *Cell Mol Biol Lett.* 2021;26(1):47.
- Murata D, Fujimoto R, Nakayama K. Osteochondral regeneration using adipose tissue-derived mesenchymal stem cells. *Int J Mol Sci.* 2020;21(10):3589.
- Ross CL, Ang DC, Almeida-Porada G. Targeting mesenchymal stromal cells/pericytes (MSCs) with pulsed electromagnetic field (PEMF) has the potential to treat rheumatoid arthritis. *Front Immunol.* 2019;10:266.
- Chen X, Wang Q, Li X, Wang Q, Xie J, Fu X. Heat shock pretreatment of mesenchymal stem cells for inhibiting the apoptosis of ovarian granulosa cells enhanced the repair effect on chemotherapy-induced premature ovarian failure. *Stem Cell Res Ther.* 2018;9(1):240.
- Song Y, Dou H, Li X, Zhao X, Li Y, Liu D, Ji J, Liu F, Ding L, Ni Y, Hou Y. Exosomal miR-146a contributes to the enhanced therapeutic efficacy of interleukin-1beta-primed mesenchymal stem cells against sepsis. *Stem Cells.* 2017;35(5):1208–21.
- Philipp D, Suhr L, Wahlers T, Choi YH, Paunel-Gorgulu A. Preconditioning of bone marrow-derived mesenchymal stem cells highly strengthens their potential to promote IL-6-dependent M2b polarization. *Stem Cell Res Ther.* 2018;9(1):286.
- Li C, Huang J, Zhu H, Shi Q, Li D, Ju X. Pyridoxal-5'-phosphate promotes immunomodulatory function of adipose-derived mesenchymal stem cells through indoleamine 2,3-dioxygenase-1 and TLR4/NF-kappaB pathway. *Stem Cells Int.* 2019;2019:3121246.
- Davis S, Meltzer PS. GEOquery: a bridge between the Gene Expression Omnibus (GEO) and BioConductor. *Bioinformatics.* 2007;23(14):1846–47.
- Kiehn JT, Tsang AH, Heyde I, Leinweber B, Kolbe I, Leliavski A, Oster H. Circadian rhythms in adipose tissue physiology. *Compr Physiol.* 2017;7(2):383–427.
- Ravi M, Paramesh V, Kaviya SR, Anuradha E, Solomon FD. 3D cell culture systems: advantages and applications. *J Cell Physiol.* 2015;230(1):16–26.

22. Nowak-Sliwinska P, Segura T, Iruela-Arispe ML. The chicken chorioallantoic membrane model in biology, medicine and bioengineering. *Angiogenesis*. 2014;17(4):779–804.
23. Rovithi M, Avan A, Funel N, Leon LG, Gomez VE, Wurdinger T, Griffioen AW, Verheul HMW, Giovannetti E. Development of bioluminescent chick chorioallantoic membrane (CAM) models for primary pancreatic cancer cells: a platform for drug testing. *Sci Rep*. 2017;7:44686.
24. Hyde KJ, Schust DJ. Immunologic challenges of human reproduction: an evolving story. *Fertil Steril*. 2016;106(3):499–510.
25. Holzmann P, Niculescu-Morzsa E, Zwickl H, Halbwirth F, Pichler M, Matzner M, Gottsauner-Wolf F, Nehrer S. Investigation of bone allografts representing different steps of the bone bank procedure using the CAM-model. *ALTEX*. 2010;27(2):97–103.
26. Presta M, Foglio E, Churrua Schuind A, Ronca R. Long pentraxin-3 modulates the angiogenic activity of fibroblast growth factor-2. *Front Immunol*. 2018;9:2327.
27. Fukushima T, Uchiyama S, Tanaka H, Kataoka H. Hepatocyte growth factor activator: a proteinase linking tissue injury with repair. *Int J Mol Sci*. 2018;19(11):3435.
28. Watanabe Y, Tsuchiya A, Seino S, Kawata Y, Kojima Y, Ikarashi S, Starkey Lewis PJ, Lu WY, Kikuta J, Kawai H, Yamagiwa S, et al. mesenchymal stem cells and induced bone marrow-derived macrophages synergistically improve liver fibrosis in mice. *Stem Cells Transl Med*. 2019;8(3):271–84.
29. Li X, Zhang Y, Liang Y, Cui Y, Yeung SC, Ip MS, Tse HF, Lian Q, Mak JC. iPSC-derived mesenchymal stem cells exert SCF-dependent recovery of cigarette smoke-induced apoptosis/proliferation imbalance in airway cells. *J Cell Mol Med*. 2017;21(2):265–77.
30. Zhang Y, Guo L, Han S, Chen L, Li C, Zhang Z, Hong Y, Zhang X, Zhou X, Jiang D, Liang X, et al. Adult mesenchymal stem cell ageing interplays with depressed mitochondrial Ndufs6. *Cell Death Dis*. 2020;11(12):1075.
31. Wysoczynski M, Pathan A, Moore JB, Farid T, Kim J, Nasr M, Kang Y, Li H, Bolli R. Pro-angiogenic actions of CMC-derived extracellular vesicles rely on selective packaging of angiopoietin 1 and 2, but not FGF-2 and VEGF. *Stem Cell Rev Rep*. 2019;15(4):530–42.
32. Yang C, Liu X, Zhao K, Zhu Y, Hu B, Zhou Y, Wang M, Wu Y, Zhang C, Xu J, Ning Y, et al. miRNA-21 promotes osteogenesis via the PTEN/PI3K/Akt/HIF-1 α pathway and enhances bone regeneration in critical size defects. *Stem Cell Res Ther*. 2019;10(1):65.
33. Lu L, Chen G, Yang J, Ma Z, Yang Y, Hu Y, Lu Y, Cao Z, Wang Y, Wang X. Bone marrow mesenchymal stem cells suppress growth and promote the apoptosis of glioma U251 cells through downregulation of the PI3K/AKT signaling pathway. *Biomed Pharmacother*. 2019;112:108625.
34. Eskla KL, Porosk R, Reimets R, Visnapuu T, Vasar E, Hundahl CA, Luuk H. Hypothermia augments stress response in mammalian cells. *Free Radic Biol Med*. 2018;121:157–68.
35. Liu X, Ren W, Jiang Z, Su Z, Ma X, Li Y, Jiang R, Zhang J, Yang X. Hypothermia inhibits the proliferation of bone marrow-derived mesenchymal stem cells and increases tolerance to hypoxia by enhancing SUMOylation. *Int J Mol Med*. 2017;40(6):1631–38.
36. Leegwater NC, Bakker AD, Hogervorst JM, Nolte PA, Klein-Nulend J. Hypothermia reduces VEGF-165 expression, but not osteogenic differentiation of human adipose stem cells under hypoxia. *PLoS ONE*. 2017;12(2):e0171492.
37. Lian Q, Zhang Y, Liang X, Gao F, Tse HF. Directed differentiation of human-induced pluripotent stem cells to mesenchymal stem cells. *Methods Mol Biol*. 2016;1416:289–98.
38. Bloor AJC, Patel A, Griffin JE, Gilleece MH, Radia R, Yeung DT, Drier D, Larson LS, Uenishi GI, Hei D, Kelly K, et al. Production, safety and efficacy of iPSC-derived mesenchymal stromal cells in acute steroid-resistant graft versus host disease: a phase I, multicenter, open-label, dose-escalation study. *Nat Med*. 2020;26(11):1720–25.